Journal of Petroleum
Science and Technology

An Estimation of Multiphase Relative Permeabilities in Reservoir Cores from Micro-CT Data

Ahmed Zoeir*[1], Alireza Tabatabaei Nezhad[1], and Jafar Qajar[2]

[1] Faculty of Petroleum and Natural Gas Engineering, Sahand University of Technology, Tabriz, Iran

[2] School of Chemical and Petroleum Engineering, Shiraz University, Shiraz, Iran

ABSTRACT

Prediction of porous media relative permeabilities from digital image data is of high demand nowadays when the power of the tomographic equipment is growing with an increasing order.

In this work three phase relative permeabilities are estimated with co-applying Darcy's and Stokes equations in two case studies, namely Bentheimer sandstone and Estaillades limestone which their micro-CT data files were downloaded from Imperial College website. In order to perform calculations firstly we extracted pore connected network from the micro-CT data and it is estimated fluids distribution within pore channels during two-phase flow. Then we calculated pressure distribution of each phase solving its continuity and momentum equations within the obtained connected phase network. Pressure distribution and fixed volumetric flow rate (that flows through all cross-sections perpendicular to the supposed flow direction), then were applied to solve for effective permeabilities. Effective permeabilities were then related to the relevant saturation and curves of two -phase relative permeabilities were derived in this manner. Stone's equation was finally applied to estimate three phase permeability ternary curves. Results showed that application of correlations for determining fluid distributions is accurate enough for multiphase relative permeability estimation in real case studies. This paper also shows that performing calculations on the segmented REVs is more accurate than work on simplified pore network models extracted from micro-CT data.

Keywords: Relative Permeability, Micro-CT, Multiphase Flow, Reservoir Rocks.

INTRODUCTION

X-ray micro-computed tomography (micro-CT) nowadays is widely applied for porous media characterization in the upstream oil industry. Also, the main advantage of the micro-CT technique is that it is non-destructive. Unlike the routine measurement methods in which the original properties are always slightly changed after each step, in X-ray imaging method, core samples do not expose to serious damage. In addition to that, the micro-CT technique allows us to analyzing friable and unconsolidated cores, sidewall cores and core fragments. In addition,

***Corresponding author**
Ahmed Zoeir
Email: ah_zoeir@sut.ac.ir
Tel: +98 41 3344 9150
Fax: +98 41 3344 4355

Article history
Received: March 27, 2018
Received in revised form: July 10, 2018
Accepted: July 16, 2018
Available online: May 21, 2019
DOI: 10.22078/jpst.2018.3237.1516

rapidity and cost effectiveness of the micro-CT method have motivated investigators in recent decades to apply scanning and numerical calculation techniques instead of physical measurements. Moreover, CT scanning technique can provide valuable information about fluid flow through porous media, e.g. in IOR/EOR research and also core sample characterization, particularly absolute and relative permeabilities. To perform precise numerical calculations on dynamic properties, the internal structure of the porous media needs to be known via 2D thin section data or 3D CT scan data [1]. Moreover, the current state of art is to image the dry core sample and to compute the petrophysical properties of interest from the provided data. Permeability is inherently a function of the internal structure of the rock sample, i.e. it mainly depends on tortuosity, pore aspect ratio and topology. However, no exact relationship exists to correlate permeability of real rocks to such static parameters, although several simplified correlations have been proposed [2]. Therefore, the fundamental mass conservation and transport equations must be solved, and it is attempted to capture relevant physics at the pore scale directly on the image or simplified representations of connected pore network. Although network models simplify the complex geometry and topology of pore structures, they are still unable to capture complex geometrical features of the original pore structure [3]. Moreover, success in techniques of predicting dynamic properties like relative permeabilities and residual saturation is less certain in comparison with static porous media properties. Also, predicted relative permeabilities depend on computed fluid distributions which in turn depend on assigned the contact angles [3]. Indeed, the contact angle is commonly treated as an adjustable parameter to fit calculated permeabilities with those obtained from laboratory measurements [4]. Limited available imaging resolution and also the existence of uncertainty within fluid distribution calculation were the reasons which a few studies were directed to focus on the determination of relative permeabilities from micro-CT data [5]. Moreover, specifying wettability from image processing methods at the pore scale especially in the presence of clays and complex mineralogy is poorly understood. Predictive values of the models are also limited to clean homogeneous media and strongly wetting conditions where it is reasonable to assume a uniform contact angle throughout the porous media [6]. Various pore scale models and computational methods employed to estimate porous media dynamic properties in single and multiphase situations have been reviewed by Blunt et al and Sheppard et al [7-8]. One of the first studies to compute relative permeabilities from imaging methods has been reported by Auzerais et al. Endpoint oil relative permeabilities were calculated at fixed residual water saturation [9]. However, it seems that underestimated the laboratory measurements are underestimated by Auzerais et al due to several reasons including finite element size effects, discretization errors and static fluctuations [2]. On average, two-phase relative permeabilities which were obtained from segmented layered data sets were reported by Silin and Patzek. These segments came from partitioning of the full micro-CT image into layers of fixed thickness. Moreover, it is explained by Silin and Patzek that this approach reduces computational requirements while at the same time increases uncertainty within the results [5]. Oil/water two-phase relative permeabilities in

porous media was estimated by Shabro et al, and the comparison of different models rather than the comparison among results attained from models and those from measurements was reported by Shabro et al [10].

In the studies mentioned above, zero degrees contact angle was assigned to the calculations that mean the assumption of strong wettability for core samples which is not valid in most of the cases. In this regard, multiphase flow in 3D geometries was simulated by Martys et al, and assigned a non-zero contact angle to predict relative permeabilities via lattice Boltzmann method was assigned by Martys et al [11]. Two-phase relative permeability curves were directly estimated from core sample digital images with considering non-zero contact angle by Ramstad et al [12]. Two-phase relative permeability curves for water wet and mixed wet rocks using pore scale calculations via lattice Boltzmann method were predicted by Landry et al [13]. It is reported by Blunt et al that assigning a non-zero contact angle in relative permeability estimation will increase the uncertainty within the results [7]. It is presented by Hussain et al that uncertainties decrease when using imaged fluid distribution in relative permeability calculations rather than predicting fluid distribution in porous space via correlations [14]. The non-wetting phase relative permeability on experimentally generated fluid distributions within porous media has been computed by Turner et al. This method removes the limitation associated with wettability is removed by this method due to the fact that generated distributions have represented real wettability conditions. An excellent match of computational results and laboratory data previously reported in the literature has been found by them [15]. Turner's works and performed steady state drainage experiments on Bentheimer sandstone core sample have been extended by Hussain et al. After each equilibrium state, core sample was removed from the experimental facility and was transported for imaging. The obtained fluid distributions were then used to compute relative permeabilities. However, removing the core sample from experimental facility resulted in the underestimation of relative permeability values [14]. Oil/water relative permeability curves for an imbibition process in a sandstone core sample which was imaged using X-ray synchrotron was estimated by Berg et al. Calculational results were then compared with those obtained from water imbibition process that was performed on the twin of that core in the laboratory. While the resultant curves showed a good agreement with the experimental data, end point relative permeabilities were deviated about 10%. It has been concluded that the phase discontinuity is the source of this uncertainty [16]. Oil/water relative permeabilities in core samples with a wide range of pore sizes have been estimated by Bultreys et al. Two sandstone cores and three carbonate cores were included in X-ray micro-CT imaging procedure, and pore scale models were developed for each one. Then relative permeabilities and capillary pressure curves were estimated in each developed model [17].

In this paper, the gas/oil/water three phase permeabilities in Bentheimer sandstone and Estaillades limestone case studies which their micro-CT data files were downloaded from the Imperial College website were estimated [18]. The oil/water and gas/oil two-phase relative permeability curves were calculated from solvation of Stokes equation in the extracted connected phase network within the case studies, with respect to oil/water and gas/

oil two phase fluid distributions in each pore. Then the Stone's equation was applied to obtain three phase relative permeability ternary diagrams from two-phase relevant relative permeability curves. For performing these calculations, an in-house program was developed by us using MATLAB R2015 software to analyze the downloaded NHDR files and to calculate porous media static and dynamic properties. The novelty of this study compared with all previous work in literature is that multiphase relative permeabilities were calculated (by us) for drainage and imbibition conditions with adjusting reported different average contact angles for each process. In addition to that, since investigators normally use pore network modelling to simplify complex porous media internal structure, another difference of this investigation with such studies is that the need for this time consuming process via reducing data volume is eliminated by us. Our recommended solution to prevent increscent in calculational runtime is working on REVs instead of full data. Calculated results are in a good agreement with values reported from SCAL. Anyway, always, there are sources of uncertainty within each calculation performed on micro-CT data. Moreover, limited imaging power restricts us to provide high resolution images which can fully explain porous media. In addition to that reducing volume of data to REV in order to efficiently use computational resources will increase uncertainties within the results. Furthermore any possible discontinuity of wetting or non-wetting phases near the connate and residual saturations can disturb calculation of relative permeability curves.

EXPERIMENTAL PROCEDURES

Computational Methodology

In this paper , the three phase relative permeabilities are estimated by us using digital micro-CT image data of two core samples, Bentheimer sandstone and Estaillades limestone. In order to minimize runtime of processes, our calculations on segmented micro-CT data with the size of permeability REV (representative elementary volume) were performed by us. To obtain permeability REV from the micro-CT data, a growing cubic control volume was supposed within the porous media which started expanding from one fixed voxel in the 3D digital image, and its dimensions increased continuously while its absolute permeability was determined at the same time. When the calculated value of absolute permeability, converged to a fixed value with a certain tolerance, the volume expansion terminated and the resulting volume is reported as the permeability REV.

In this paper, micro-CT data in the medical format of NHDR (same as NRRD) which then is imported into MATLAB R2015 software were used by us. In order to use the predefined functions and modules of the Image Region Analyzer of MATLAB R2015 for the NHDR files, the 3D micro-CT data into series of 2D data was converted by us. Several static properties of porous media are calculated using MATLAB's Image Region Analyzer APP. For porosity calculation, the MATLAB mask is applied to divide voxels into two groups of pores and solids. Moreover, the function's threshold to fit the reported porosity from the RCAL experiment was adjusted by us in order to calibrate the micro-CT data and use it for calculation of relative permeabilities. Pores within the 2D data are equalized with circles with the same area, and the resulted diameters are used to calculate pore size distribution curve. The contact area of solid and fluid phases is determined in each 2D section and is multiplied with voxel width and then is added to other section's contact areas to give

overall contact area within the full 3D image. After that, we used the morphological reconstruction abilities of MATLAB's Image Region Analyzer APP to extract connected pore network from 3D micro-CT images. The set connection degree governed that each pore voxel could neighbor up to six other pore voxels on each face of the cube, not on the edges or corners. After the elimination of the isolated pores, remaining voxels construct the connected pore network. In order to estimate two phase relative permeabilities of water/oil and oil/gas, firstly, wetting and non-wetting phase distributions within the extracted connected pore network were calculated by us within two case studies. Bentheimer sandstone represents water wet behaviour while Estaillades limestone is oil wet.

Phase distributions were calculated for an extent of saturation, ranged from connate of one phase to the residual of the other phase. In each overall saturation, we estimated the space occupied with each phase within each pore with this assumption that average saturation in each cross section perpendicular to flow direction is equal to overall saturation.

To calculate the space occupied with phases within each pore, right angle MS-P (Mayer-Stowe-Princen) method has been applied which considers the capillary forces as dominant and neglects the gravity forces [19]. For an interface with moderate curvature, where the radius of curvature is much smaller than the width of the interface, each fluid's free energy differential is expressed as [19].

$$dF = -SdT + \sum_i \mu_i dn_i + \gamma dA \quad (1)$$

The system is in equilibrium; therefore, the total change in the free energy is zero. In addition, temperature and component's chemical potential are constant, so [19].

$$dF_T = dF_w + dF_{nw} + dF_{w,n\,w} + dF_{w,s} + dF_{nw,s} = 0$$

$$(P_{nw} - P_w)dV_{nw} = \gamma dA_{w,nw} + \gamma_{nw,s}\, dA_{nw,s} + \gamma_{w,s}\, dA_{w,s} \quad (2)$$

Relating variations of the interfacial area to contact perimeters of phases and grains gives [19].

$$dA_{nw,s} = -dA_{w,s} = Peri_{nw,s}\, dL$$

$$dA_{nw,w} = Peri_{nw,w}\, dL \quad (3)$$

The interfacial tension forces between non-wetting, wetting and solid phases are related with the contact angle, therefore, the final MS-P formula for right angle duct is formed as [19].

$$P_c = \frac{\gamma\left(Peri_{nw,w}\cos\theta + Peri_{nw,s}\right)}{S_{nw}} \quad (4)$$

Figure 1 shows a schematic representation of a 2D segmented cross section of a channel within connected pore network of Bentheimer sandstone. Non-wetting phase pressure is higher than pore's entrance threshold pressure thus channel's cross section which consists of four voxels contains both wetting and non-wetting phases.

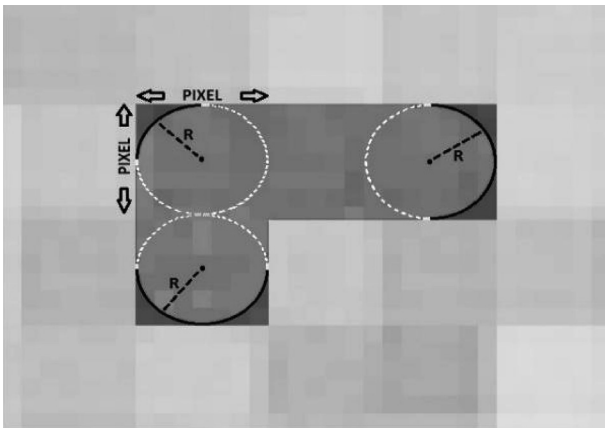

Figure 1: 2D schematic segmented cross section of a channel within the connected pore network.

During the calculation of two phase relative permeabilities from micro-CT data, all cross sections of channels within the connected pore network only contain similar right angle corners because the voxels of digital images are perfect cubes. To

estimate the space occupied with each phase within the connected pore network it is assumed that sectional saturation is equal to overall saturation. In addition, regarding small pores in each section in which non-wetting phase pressure cannot overcome capillary pressure, not allowing non-wetting fluid to enter such pores. Also, there are always some differences between saturations in larger pores within same section and the overall saturation. Anyway saturation in such larger pores have been normalized to give fixed sectional saturations. After the estimation of space occupied with each phase within 2D cross sections of channels, spaces were connected to form a 3D connected phase network. A pressure differential is superimposed across the faces of the micro-CT data orthogonal to the axis of core sample case study and the corresponding flow rate is computed assuming no-flow conditions for other faces of the core sample and no-slip condition at the solid-fluid interfaces. The velocity field is determined by to solve Stokes and mass conservation equations in the digitized image data. To aim this, the pore network cross sections as closed ducts and calculated their average hydraulic diameters in spaces occupied with wetting and non-wetting phases were treated by us. In reality pore voxels that are in contact with the solid phase represent no-slip condition while those located in the center of pore have the largest linear velocities. To adjust this effect, we used the Euclidean Distance Transform as a solution to this conflict was used by us. It assigns zero number to pore voxels which are in contact with the solid phase, and larger numbers to pore voxels which are farther from solid phase. This number grows as voxel distance from solid phase increases.

Velocity distribution in all points of porous media was obtained by multiplying distance transform numbers with linear velocities calculated from the Stokes equation. Effective permeabilities were then computed using Darcy's law. Calculations were performed for two conditions, drainage process in which non-wetting phase is injected into porous media and the imbibition process in which wetting phase saturation is increasing in media. Two different values were reported for the average contact angle for each process in Bentheimer sandstone and Estaillades limestone case studies. The contact angle as a fixed value within all sections perpendicular to the supposed flow direction was adjusted by us. Because of relative cleanness and homogeneity of Bentheimer sandstone and Estaillades limestone and also regarding strong wettability behavior of core samples, this assumption seems reasonable.

Several realizations with different saturations were performed to firstly estimate phase distributions and then to calculate two phase relative permeabilities of water/oil and gas/oil within Bentheimer sandstone and Estaillades limestone. Finally, Stone's equation was used to combine two-phase relative permeability curves and calculate three phase relative permeabilities. An in-house code has been written with MATLAB R2015 using its Image Region Analyzer APP to the calculated core properties from micro-CT data, as is shown in Figure 2. Our written MATLAB code is capable to calculate absolute and connected porosities, pore, and throat size distributions, REVs of porosity and permeability, absolute and two and three phase relative permeabilities from the micro-CT data in NC, NRRD, NHDR, and DICOM formats.

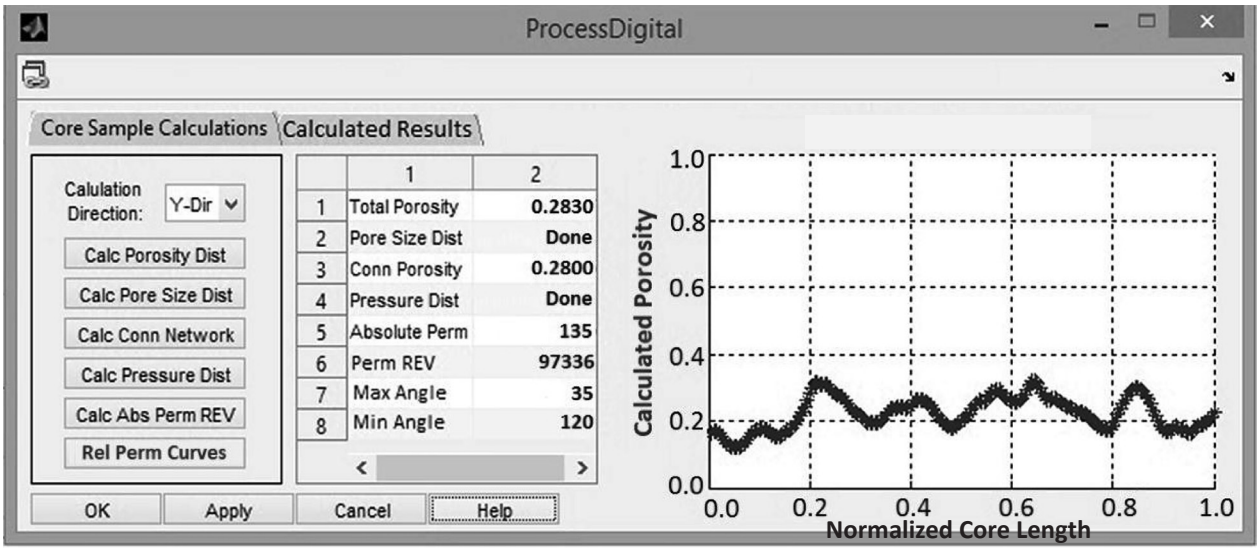

Figure 2: An image of the developed MATLAB GUI code to calculate core properties from micro-CT data.

RESULTS AND DISCUSSIONS

In the first stage of the computational procedure, the representative elementary volumes of porosity and permeability are required to calculate porous media properties. In this regard, some random voxels were selected within the micro-CT image of the core sample case studies, each one as a growing control volume. Then the volume of each selected voxel was expanded and the corresponding porosity, and permeability values were calculated. The increase in of volume size continues until finally the calculated porosity and permeability reach to relatively constant values. The volume corresponds to such constant values of porosity, and permeability were considered as the REVs. By knowing REVs, which are several times smaller than full micro-CT data, we segmented some volumes within downloaded micro-CT data, which were slightly larger than REV volumes, firstly, to ensure representativeness of the calculated properties, and secondly to reduce runtime and RAM requirements. Average values of calculated properties within all segmented volumes, are presented in Table 1 and also are compared with the reported values for Bentheimer sandstone and Estaillades limestone case studies.

Table 1: Calculated versus reported properties of Bentheimer sandstone and Estaillades limestone case studies.

Porous Media Property		Connected Porosity (%)	Ave Pore Size (μm)	Ave Throat Size (μm)	ABS Perm REV (μm^3)	ABS Perm (mD)
Bentheimer Sandstone	Calculated	23.2	13.0	8.0	450000	2650
	Reported	24.0	15.0	10.0	512000	2800
Estaillades Limestone	Calculated	28.3	8.0	4.0	100000	135
	Reported	29.0	10.0	5.0	125000	150

As demonstrated in Table 1, the average calculated porosities from micro-CT data processing with values of 23.2% and 28.3% respectively for Bentheimer sandstone and Estaillades limestone show good agreement with the reported experimental value of 24.0% and 29.0%. Relative error for porosity calculation is only 3% in Bentheimer sandstone and 4% in Estaillades limestone case studies. Similarly, the absolute permeability values obtained from micro-CT data processing on relevant REVs, 2650 mD and 135 mD for Bentheimer sandstone and Estaillades limestone case studies, are also close to reported values of 2800 mD and 150 mD and show relative error of 5% and 10% respectively. Pore size distribution curves were extracted from downloaded NHDR data files of Bentheimer sandstone and Estaillades limestone using written In-house MATLAB R2015 code, and their average pore and throat sizes are reported as shown in Table 1.

In order to estimate the two phase relative permeability curves of oil/water and gas/oil within Bentheimer sandstone, a series of saturation were assigned to permeability REV. Then the distribution of each phase was estimated for each individual pore or channel within the connected pore network. Wetting and non-wetting phase volumes were considered to connect to each other from one section to another, and the resultant networks were supposed to form connected phase networks. After construction of a connected phase network, Stokes' equation was solved for each phase network, and the effective permeabilities were calculated for every assigned saturation. Estimated effective permeabilities were then divided with absolute permeability value and were used in Corey (or LET) type curve fitting process to give curves as demonstrated in Figure 3.

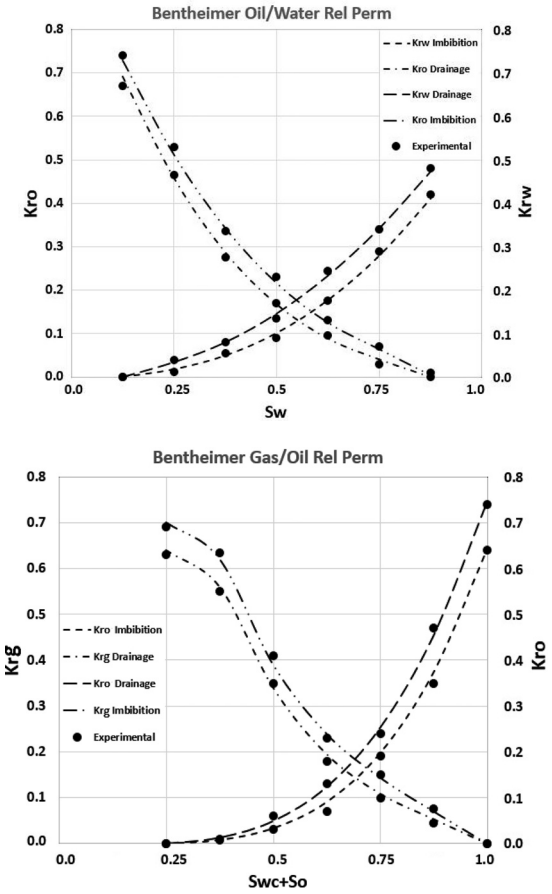

Figure 3: Estimated two-phase relative permeability curves within Bentheimer sandstone case study.

Corey type correlations are used to obtain relative permeability curves of water and oil while LET type curves are used to correlate gas relative permeability data. The reason to do this is that the calculated and also the reported values of gas permeability show decelerational increase near the irreducible fluid saturation. Moreover, calculated two-phase relative permeability curves of oil/water and gas/oil are in good agreement with the reported experimental data. The relative permeability estimations were performed for two processes of drainage and imbibition within Bentheimer sandstone case study. Contact angle between wetting and non-wetting fluids were adjusted according to the reported average value for the calculation of phase distributions. During

drainage process in water wet Bentheimer core sample oil relative permeabilities are lower than that of imbibition process. Conversely water relative permeabilities in drainage process are higher than imbibition. That's the reason for the difference between relative permeability curves of water and oil in drainage and imbibition processes in Bentheimer sandstone case study. Bentheimer sandstone represents water wet behavior while conversely the Estaillades limestone is slightly oil wet. In order to estimate two phase relative permeability curves of oil/water and gas/oil in Estaillades limestone, again some series of saturations were assigned to permeability REV. Then the distribution of each phase was estimated for each individual pore or channel within the connected pore network. Wetting and non-wetting phase volumes were considered to connect to each other from one section to another perpendicular to supposed flow direction, and the resultant networks were assumed to form connected phase networks. After connected phase network construction, Stokes' equation was solved for each phase network, and the effective permeabilities were calculated for every assigned saturation. Estimated effective permeabilities were then divided with absolute permeability value and were used in Corey (or LET) type curve fitting process to give curves as demonstrated in Figure 4.

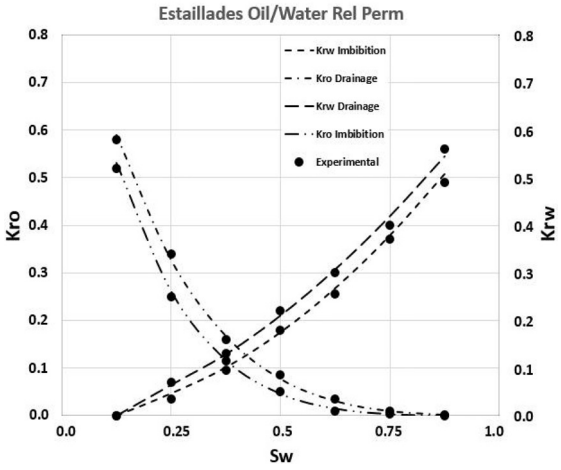

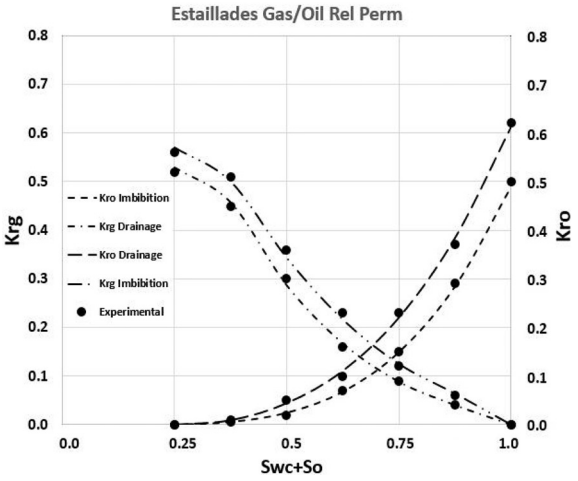

Figure 4: Estimated two-phase relative permeability curves within Estaillades limestone case study.

As shown in Figure 4, Corey type curve fittings are used to correlate relative permeabilities of water and oil while LET type curves are used to correlate the gas relative permeability data. In addition, reported experimental data again are shown with dark segregated points in Figure 4.

Calculated two-phase relative permeability curves of oil/water and gas/oil are in a good agreement with the reported data. Relative permeability estimations were performed for two processes of imbibition and drainage. The only difference in calculations relevant to each process was again that the contact angle input parameter was adjusted according to the reported average value to obtain phase distributions. During the drainage process in oil wet core sample, oil relative permeabilities were higher than that of imbibition process. Conversely, water relative permeabilities in the drainage process were higher than imbibition. That's the reason for the difference between relative permeability curves of water and oil in drainage and imbibition processes in Estaillades limestone case study. In order to estimate three phase relative permeability curves within Bentheimer sandstone and Estaillades carbonate, Stone's

equation and two-phase relative permeabilities as input data were used by us. Stone's equation considers wetting phase (water in Bentheimer sandstone and oil in Estaillades limestone) and the gas phase permeability curves similar to that of the two-phase condition. Non-wetting liquid phase (oil in Bentheimer and water in Estaillades limestone) permeabilities were then calculated from permeability values of other phases. As relative permeabilities in three phase conditions are functions of oil, water, and gas saturation, results are presented in ternary diagrams. Calculated results for Bentheimer sandstone in drainage and imbibition processes are introduced in Figure 5.

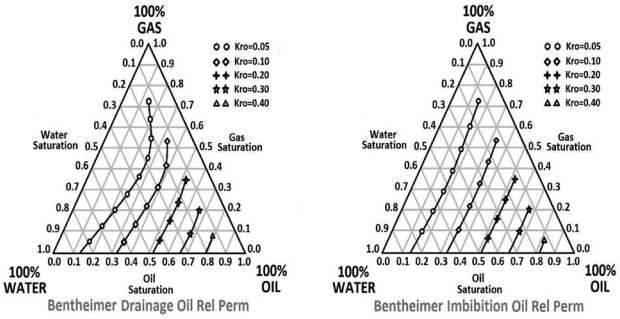

Figure 5: Estimated three-phase relative permeability ternary curves within Bentheimer sandstone.

Curves do not cover regions in ternary diagram in which water or oil saturations are smaller than corresponding irreducible values. Higher oil relative permeabilities take place in situations with higher oil saturation and minimum (zero) gas saturation. As oil saturation is reduced within porous media, oil relative permeabilities are decreased with an increasing order. Oil relative permeabilities within Bentheimer sandstone case study rarely reach 0.5 even at highest oil saturation. Also, calculated results showed that during drainage process, oil effective permeabilities are lower than effective permeabilities under the imbibition process. Oil saturation has more influence on this behavior at lower values and loses its effect in higher saturation. Same calculations were performed for Estaillades limestone oil wet case study. Results are presented in Figure 6.

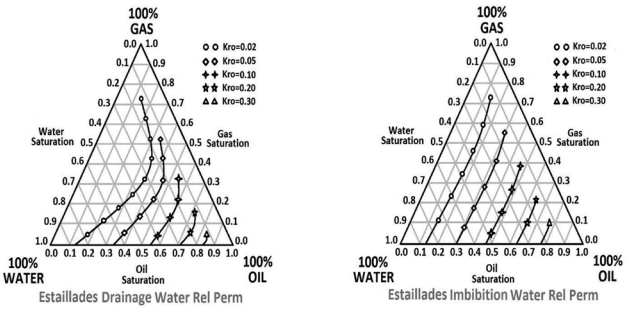

Figure 6: Estimated three phase relative permeability ternary curves within Estaillades limestone.

As demonstrated in Figure 6, again relative permeability curves do not cover those regions in ternary diagram in which water or oil saturations are smaller than corresponding irreducible values. Higher oil relative permeabilities take place in situations with higher oil saturation and minimum water and gas saturation. As oil saturation increases within porous media, oil relative permeabilities increase with a decelerating order. Oil relative permeability curves within Estaillades limestone case study rarely exceed 0.4 even at highest oil saturation. Calculated results showed that oil effective permeabilities during imbibition process were higher than effective permeabilities under drainage process. Oil saturation has more influence on this behavior at lower values and loses its effect in higher saturation. Unfortunately, the three-phase relative permeability values were not reported experimentally in for the taken case studies.

The results showed that it is recommendable to present that one can calculate dynamic properties of porous space via well understanding the internal structure of media with the aid of micro-CT imaging. Macroscopic flow equations can be

applied to extracted connected phase network to give accurate enough relative permeabilities in multiphase flow. This can aid petroleum engineers to apply non-destructive cost effective X-ray imaging and processing methods to estimate dynamic properties of porous media, instead of conventional costly SCAL experiments.

CONCLUSIONS

Several key findings of the present paper can be summarized as follows:

1. Calculation of dynamic properties of porous materials from understanding media's internal structure and extraction of connected pore network gives an acceptable results which are in good agreement with experimental results.
2. Accurate estimation of three phase relative permeabilities within clean core samples like Bentheimer sandstone and Estaillades limestone takes place with solving macroscopic flow equations for the extracted connected phase network.
3. The existence of impurities like clay within reservoir cores will increase uncertainty within the results. Relative permeabilities are influenced with non-uniqueness of contact angle in all point of porous media.
4. (Hysteresis effects will influence multiphase relative permeability curves in the same trend as they affect two phase curves. Physically connected phase network is different at drainage and imbibition processes and leads to different calculations in the same saturation.
5. In processing 3D digital images with MATLAB, if possible, it is advised by us reducing input data amount to representative elementary volume (REV) of permeability to avoid additional unnecessary RAM usage. Also, in coding procedures, if needed, it is recommended not to define multidimensional matrixes which are larger than the original image size. It is recommended to use unavoidable input data as the largest matrix in the program.
6. The fastest procedure of digital image processing in MATLAB takes place when working with its Image Region Analyzer's predefined functions. Determining the contact area, providing a connected pore network, Euclidean distance transform mapping and calculation of representative volumes, all have predefined functions in Image Region Analyzer module of MATLAB R2015. Make sure your desired function is not available by default before trying to write your own function.

ACKNOWLEDGEMENTS

The authors acknowledge the free support of micro-CT images by the Imperial College Website, London, England.

NOMENCLATURES

CT	: Computed Tomography
REV	: Representative Element Volume

REFERENCES

1. Dong H. and Blunt M. J., "Pore Network Extraction from Micro Computerized Tomography Images," *Physical Review E*, **2009**, *80*, 36307-36318.
2. Arns C. H., Knackstedt M. A., Pinczewski M. V., and Lindquist W. B., "Accurate Estimation of Transport Properties from Microtomographic Images," *Geophysical Research Letters*, **2001**, *28*, 3361-3364,.
3. Ramstad T., Oren P. E., and Bakke S., "Simulation

of Two Phase Flow in Reservoir Rocks Using a Lattice Boltzmann Method," *SPE Journal*, **2010**, *15*, 917-927.

4. Sorbie K. S. and Skauge A., "Can Network Modeling Predict Two-phase Flow Functions?," *Petrophysics*, **2012**, *53*(06), 401-409.
5. Silin D. B. and Patzek T. W., "Predicting Relative-permeability Curves Directly from Rock Images," *SPE Annual Technical Conference and Exhibition*, New Orlean, Louisiana, USA, **2009**.
6. Jin G., Radaelli F., and Rossi E., "Experimental Validation of Pore-level Calculations of Static and Dynamic Petrophysical Properties of Clastic Rocks," *SPE Annual Technical Conference and Exhibition*, California, **2007**.
7. Blunt M. J., Dong B., Mostaghimi P., and GHarbi O., "Pore-scale Imaging and Modelling," *Advances in Water Resources*, **2013**, *51*, 197-216.
8. Wildenschild D. and Sheppard A. P., "X-ray Imaging and Analysis Techniques for Quantifying Pore-scale Structure and Processes in Subsurface Porous Media Systems," *Advances in Water Resources*, **2013**, *51*, 217-246.
9. Auzerais F. M., Dunsmuir J., Ferreol B. B., Martys N., and et al., "Transport in Sandstone: A Study Based on Three Dimensional Microtomography," Geophysical Research Letters, **1996**, *23*, 705-708.
10. Shabro V., Prodanovic M., and Farzam Javadpour., "Pore Scale Modeling of Two Phase Flow," *Eighteenth International Conference on Computational Methods in Water Resources*, Barcelona, Spain, **2010**.
11. Martys N. S. and Chen H., "Simulation of Multicomponent Fluids in Complex Three-dimensional Geometries by the Lattice Boltzmann Method," *Physical Review E*, **1996**, *53*, 743-750.
12. Ramstad T., Idowu N., Nardi C., and Oren P. E., "Relative Permeability Calculations from Two Phase Flow Simulations Directly on Digital Images of Porous Rocks," *Transport in Porous Media*, **2012**, *94*, 487-504,.
13. Landry C. J., Karpyn Z. T., and Ayala O., "Relative Permeability of Homogenous-wet and Mixedwet Porous Media as Determined by Pore-scale Lattice Boltzmann Modeling," *Water Resources Research,* **2014**, *50*, 3672-3689.
14. Hussain, F., Zou Sh., Arns J., Guo Zh., and et al., "Computation of Relative Permeability from Imaged Fluid Distributions at the Pore Scale," *Transport in Porous Media*, **2014**, *104*, 91-107.
15. Turner M. L., Knuefing L., Arns C. H., Sakellariou A., and et al., "Three-dimensional Imaging of Multiphase Flow in Porous Media," *Physica A: Statistical Mechanics and its Applications*, **2004**, *339*(1-2), 166-172.
16. Berg S., Rücker M., Ott H., Georgiadis A., and et al., "Connected Pathway Relative Permeability from Pore-scale Imaging of Imbibition", Advances in Water Resources, **2016**, 24-35.
17. Bultreys T., Stappen J. V., Kock T. D., Boever W. D., and et al., "Investigating the Relative Permeability Behaviour of Micoporosity-Rich Carbonates and Tight Sandstones with Multi-scale Pore Network Models," *American Geophysical Union*, **2016**, *121*(11), 7929-7945.
18. Torland A., "A Pore Network Investigation of Factors Influencing the Residual Oil Saturation," Master's Thesis, NTNU, **2018**.
19. Lago M. and Araujo M., "Threshold Pressure in Capillaries with Polygonal Cross Section," *Journal of Colloid and Interface Science*, **2001**, *243*, 219-226.